



## Full Length Article

# Microstructure and mechanical properties of Ti/Al co-doped DLC films: Dependence on sputtering current, source gas, and substrate bias



Ting Guo<sup>a,c,1</sup>, Cuicui Kong<sup>a,b,1</sup>, Xiaowei Li<sup>a,\*</sup>, Peng Guo<sup>a</sup>, Zhenyu Wang<sup>a</sup>, Aiying Wang<sup>a,\*</sup>

<sup>a</sup> Key Laboratory of Marine Materials and Related Technologies, Zhejiang Key Laboratory of Marine Materials and Protective Technologies, Ningbo Institute of Materials Technology and Engineering, Chinese Academy of Sciences, Ningbo 315201, PR China

<sup>b</sup> Ningbo University, Ningbo 315201, PR China

<sup>c</sup> School of Materials Science and Engineering, Shanghai University, Shanghai 200444, PR China

## ARTICLE INFO

## Article history:

Received 30 November 2016  
Received in revised form 11 January 2017  
Accepted 28 February 2017  
Available online 1 March 2017

## Keywords:

Diamond-like carbon  
Process parameters  
Ti/Al co-doping  
Residual compressive stress  
Mechanical properties  
Hybrid ion beam technique

## ABSTRACT

Co-doping two metal elements into diamond-like carbon (DLC) films can reach the desirable combined properties, but the preparation and commercialized application of metal co-doped DLC films with well-defined structural properties are currently hindered by the non-comprehensive understanding of structural evolutions under different process parameters. Here, we fabricated the Ti/Al-DLC films using a unique hybrid ion beam system which enabled the independent control of metal content and carbon structure. The evolutions of microstructure, residual compressive stress and mechanical properties induced by the different process parameters including sputtering currents, C<sub>2</sub>H<sub>2</sub> or CH<sub>4</sub> source gases and bias voltages were investigated systematically in order to perform in-depth analysis on the relation between the structure and properties in Ti/Al-DLC films. Results revealed that the variations of process parameters seriously affected the concentration and chemical bond state of co-doped Ti/Al atoms in amorphous carbon matrix or incident energies of C ions, which brought the complicated effect on amorphous carbon structures, accounting for the change of residual compressive stress, hardness and toughness. The present results provide the guidance for suitable, effective parameters selection to tailor the Ti/Al-DLC films with high performance for further applications.

© 2017 Elsevier B.V. All rights reserved.

## 1. Introduction

It becomes highly significant to improve the performance of automobile components with the severely prominent energy sources and environmental issues, which require an eco-friendly surface treatment technology to substitute for the conventional wet electroplating process, because of the chromium-riched electrolyte. Due to the superior properties including high hardness, low coefficient of friction and chemical inertness, diamond-like carbon (DLC) films have been considered as strong candidates for the required surface treatment technology [1,2]. Such DLC films can not only enhance both the performance and lifetime of automobile components, but also offer the eco-friendly deposition processes

such as physical/chemical vapor deposition. To expand their application areas and overcome the intrinsic limitations of high residual stress, embedding single metal element into DLC matrix named as Me-DLC has been adopted, which creates a multiphase nanocomposite material exhibiting the tunable functionalities from the improved tribological properties to adhesion strength and reduced residual stress [3–5]. However, the excellent combined properties have rarely been achieved by introducing a single metal element to DLC matrix.

Recently, our ab initio calculations found that the co-doping of Ti/Al or Cu/Cr could significantly remove the intrinsic limitations of DLC films without deteriorating the mechanical properties [6,7]. Liu et al. [8] also deposited the Ti/Al-DLC films by middle frequency magnetron sputtering technique and reported that, compared with Ti-DLC films, the simultaneous introduction of Ti and Al lowered the residual compressive stress effectively and also made the films exhibiting superhigh elastic recovery, low coefficient of friction and wear rate. Moreover, co-doping Si/Al benefited the nearly fric-

\* Corresponding authors.

E-mail addresses: [lixw@nimte.ac.cn](mailto:lixw@nimte.ac.cn) (X. Li), [aywang@nimte.ac.cn](mailto:aywang@nimte.ac.cn) (A. Wang).

<sup>1</sup> These authors contributed to this work equally.

tionless and extremely elastic performance for DLC films due to the formed dual self-assembled dual nanostructures [9]. Hence, co-doping two metals into DLC structure show the potential to enhance the combined properties of DLC films to the utmost extent.

However, it is well known that the microstructure and properties of DLC films strongly depend on the deposition techniques and process parameters. Compared to the traditional methods such as filtered cathodic vacuum arc, magnetron sputtering and plasma enhanced CVD, hybrid ion beam deposition system, comprising a DC magnetron sputtering unit and an anode-layer linear ion beam source (ALIS) [10–12], not only easily tailor the metal concentrations and intrinsic carbon structure of films, but also separately facilitate the operation of high ionization rate and kinetic energy for carbon matrix. In addition, the ALIS technique owns the priorities of stable ionized plasma, large-area uniformity, as well as low temperature deposition [13,14]. So far, the studies on single metal doped DLC films which were deposited by hybrid ion beam deposition, have been well proceeded [3,5,10,11,15], but the information about two metal elements doped cases by ALIS technique was poorly undertaken.

Recently, Li et al. successfully fabricated the Ti/Al co-doped DLC films by a hybrid ion beam deposition system [16], but it mainly focused on the stress reduction mechanism caused by Ti/Al co-doping. The dependence of metal co-doped DLC films on the key process parameters including ion energy, ion density and ion features is still unclear, whereas it is absolutely prerequisite to tailor the desired properties and further provide the essential technical parameters for industrialized application. So in the present work, we took full advantage of this hybrid ion beam system to fabricate the Ti/Al-DLC films. The microstructure and properties of films were systematically studied as a function of key deposition parameters such as sputtering current, source gas and negative bias voltage, which were strongly related with deposited ion features. The in-depth analysis of composition, atomic bond structure, residual compressive stress and mechanical behavior were conducted to reveal the relation between the microstructure and properties. It was observed that the residual compressive stress, hardness and toughness of films were closely sensitive to the process parameters and the existed state of co-doped Ti/Al atoms in the amorphous carbon matrix, which provided the guidance for preparing Ti/Al-DLC films with high performance.

## 2. Experimental details

### 2.1. Film deposition

The Ti/Al-DLC films were prepared by the unique hybrid ion beam deposition system consisting of a DC magnetron sputtering with Ti/Al composite target and an ALIS supplied with hydrocarbon gas ( $\text{CH}_4$  or  $\text{C}_2\text{H}_2$ ) for DLC film deposition [3,15]. P-type Si (100) wafers with thickness of  $450 \pm 20 \mu\text{m}$  were used as substrates, and a thin Si with thickness of  $240 \pm 5 \mu\text{m}$  was also used as substrate to accurately estimate the residual compressive stress. All substrates were cleaned ultrasonically in acetone and ethanol separately, and then dried in air blow before putting them into the vacuum chamber. The distance between the substrate and ALIS or Ti/Al target was controlled to 20 cm separately. Prior to the deposition, the chamber was evacuated to a vacuum of  $2.7 \times 10^{-3}$  Pa, and the substrates were pre-cleaned for 10 min using  $\text{Ar}^+$  (40 sccm) at the pulsed bias voltage of  $-100$  V. During the film deposition process, the Ti/Al composite target with Ti/Al atomic ratio of 1:1 was used. The detailed parameters such as the kinds of hydrocarbon gas, working currents of ALIS, negative bias voltages of substrate and so on were shown in Table 1.

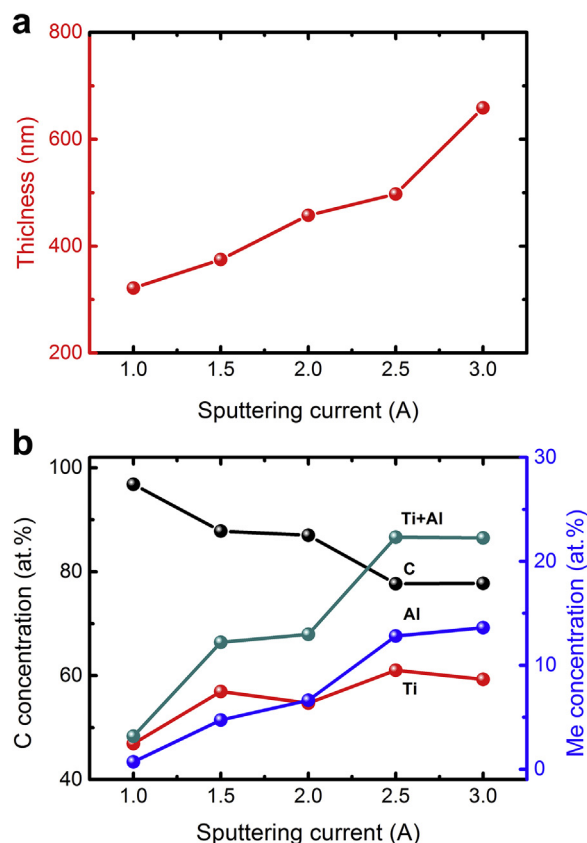


Fig. 1. (a) Thickness and (b) compositions of Ti/Al-DLC films deposited at different sputtering currents and using  $\text{CH}_4$  as source gas.

### 2.2. Film characterization

A surface profilometer (Alpha-step IQ, USA) was used to measure the thickness of the deposited films with employing a step formed by a shadow mask. X-ray photoelectron spectroscopy (XPS, Thermo Scientific ESCALAB 250) with Al X-ray source was used to characterize the composition and chemical bonds of the deposited films because each element had a unique set of binding energies. Before commencing the measurement, the sample surface was etched for 5 min by the  $\text{Ar}^+$  ion beam with energy of 3 keV to remove the contaminants; the Ti/Al/C atomic ratio was determined using the standard atomic sensitivity factors and area ratio of the C 1s to Ti 2p and Al 2p peaks in XPS spectra; the hydrogen atom concentration was not considered due to its signal intensity below the XPS detection threshold. Raman spectroscopy (inVia-reflex, Renishaw) equipped with 532 nm exciting wavelength was also applied to evaluate the carbon atomic bonds at a detecting range from 800 to  $2000 \text{ cm}^{-1}$ . Cross-sectional high-resolution transmission electron microscopy (TEM) of the films was performed on Tecnai F20 electron microscope, which was operated at 200 kV with a point-to-point resolution of 0.24 nm.

Mechanical properties were measured by the nano-indentation technique (MTS-G200) in a continuous stiffness measurement mode with a maximal indentation depth of 500 nm and a Berkovich diamond tip. The characteristic hardness of deposited films was chosen in the depth where the hardness with indentation depth was stable and not affected by the substrate. Six replicate indentations were done for each sample. The residual compressive stress was calculated according to the Stoney equation and the film/substrate curvature was determined by a laser tester (JLCST022, J&L Tech).

**Table 1**  
Deposition parameters of Ti/Al-DLC films for each case.

Parameters		Case 1	Case 2	Case 3
ALIS for DLC deposition	Hydrocarbon gas	CH <sub>4</sub>	C <sub>2</sub> H <sub>2</sub>	C <sub>2</sub> H <sub>2</sub>
	Gas flow rate (sccm)	10	10	10
	Working current (A)	0.2	0.2	0.2
	Working voltage (V)	1400 ± 50	1400 ± 50	1400 ± 50
DC Magnetron sputtering for Ti/Al co-doping	Ar flow rate (sccm)	70	70	70
	Sputtering current (A)	1–3	1–3	2.5
	Negative bias voltage (V)	–50	–50	0 to –200
	Deposition time (min)	60	60	60
Working pressure (GPa)		0.56		

### 3. Results and discussion

#### 3.1. Dependence of Ti/Al-DLC films on different sputtering currents

Many previous efforts [5–7,10] have confirmed that the structure and properties of Me-DLC films were strongly dependent on the feature and concentration of doped metal, which could be easily controlled by changing the sputtering source and current. In this section, the effect of DC magnetron sputtering current (1–3 A) on Ti/Al-DLC films was focused. CH<sub>4</sub> was selected as hydrocarbon gas to obtain the hydrocarbon ions for the deposition of DLC matrix. The detailed parameters were given in case 1 of Table 1.

Fig. 1 shows that both the thickness and Ti/Al concentrations increase with sputtering current, which attributes to the increased sputtering current enhancing the bombardment effect of Ar ions on the Ti/Al composite target and thus resulting in the increase of growth rate and Ti/Al concentrations. When the sputtering current is changed from 1 to 3 A, the thickness ranges from 321 to 659 nm (Fig. 1a), and the co-doped metal concentrations in Fig. 1b vary from 2.5 to 8.6 at.% for Ti and from 0.7 to 13.6 at.% for Al, respectively. At the sputtering current of 1.5 A, the concentrations of doped Ti and Al are 7.5 and 4.7 at.% separately.

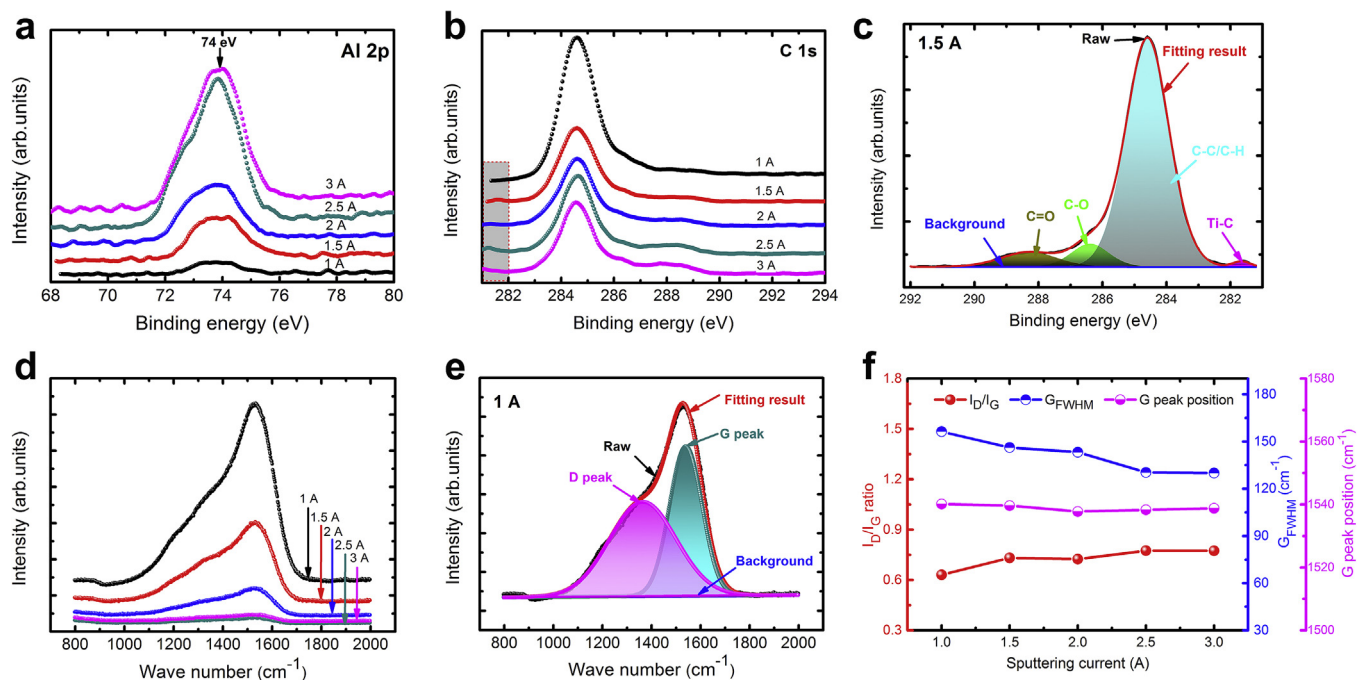
Fig. 2a–c shows the bonding structure of Ti/Al-DLC films deposited at different sputtering currents by XPS spectroscopy. After removing the easily formed metallic oxide contaminations by the Ar<sup>+</sup> bombardment, the peak position of XPS Al 2p spectra, as shown in Fig. 2a, is about 74 eV, corresponding to the Al–O bond. But it can also be observed for the existence of shoulder peak located at 73 eV in Fig. 2a, These imply that the doped Al element mainly exists in the state of pure Al nanoparticulates and oxidized Al clusters [17–19]. Fig. 2b shows the XPS C 1s spectra, where a major peak is found at around 284.6 eV originating from amorphous carbon. However, noted that the peak intensity with sputtering current decreases gradually due to the decreased C concentration in the films. When the sputtering current is higher than 1.5 A (Fig. 2c), the C 1s spectra can be fitted into four components at the binding energies of 288.3 eV for C=O bonds, 286.4 eV for C–O bonds, 284.6 eV for C–C/C–H bonds, and 281.8 eV for a small shoulder peak which has been proved to be C–Ti bonds by previous reports [20,21]. The presence of C–Ti peak indicates that the doped Ti atoms at the sputtering current of 1.5 A involve to interact with carbon atoms and thus form titanium carbides. Nevertheless, when the current is lower than 1.5 A, the doped Ti atoms are only dissolved in the amorphous carbon matrix.

Raman spectroscopy is employed to deduce the carbon atomic bonding structure, as shown in Fig. 2d. All the spectra display the typical characteristics of intrinsic DLC film, where an asymmetric scattering curve is visible [1]. However, increasing the sputtering current leads to the decrease of intensity in Raman spectra, because of the increased fraction of centrosymmetric phases, such as titanium carbides, which are inactive to the Raman excitation. It is well known that the Raman spectra can be fitted into two Gaussian

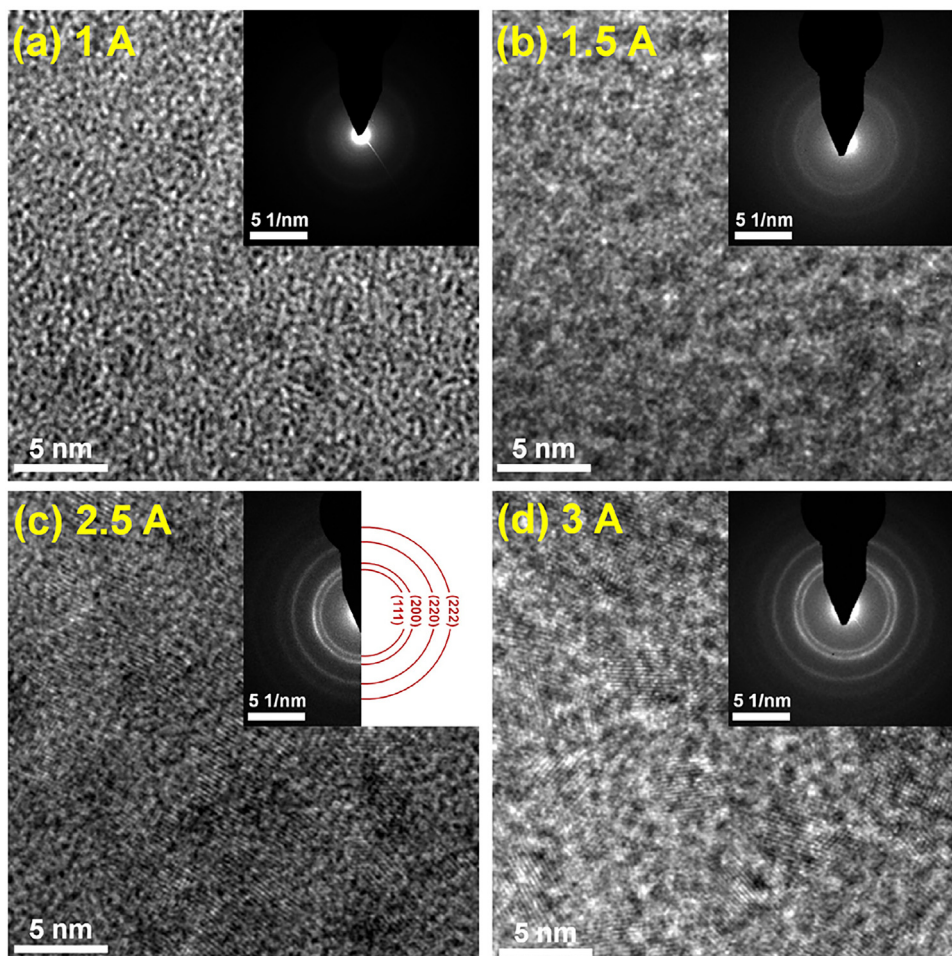
peaks (Fig. 2e), in which D peak is located at around 1360 cm<sup>–1</sup> due to the breathing mode of only sp<sup>2</sup> atoms in aromatic rings, and G peak is located at around 1540 cm<sup>–1</sup> originated from the stretching mode of sp<sup>2</sup> atoms in both aromatic rings and chains [1]. The intensity ratio of D peak to G peak (I<sub>D</sub>/I<sub>G</sub>), G peak position, and full width at half maximum of the G peak (G<sub>FWHM</sub>) can be used to evaluate the carbon atomic structure. Fig. 2f shows that there is no obvious change of the G peak with sputter current, but the I<sub>D</sub>/I<sub>G</sub> increases slightly and then reaches to a stable value. However, noted that the G<sub>FWHM</sub> related with the disorder degree of carbon structure decreases monotonously, implying the enhanced structural ordering of the film. Based on the abovementioned comprehensive analysis, it could be concluded that changing the sputtering current from 1 to 3 A results in the increase of sp<sup>2</sup> content in Ti/Al co-doped films. Choi et al. [22] have revealed that the addition of Al into carbon structures could induce the change of carbon bonding structures from sp<sup>3</sup> to sp<sup>2</sup>, and thus the catalyzing effect caused by Al with fast increased concentration (Fig. 1b) mainly contributes to the evolution of hybridization structure.

Fig. 3 shows the TEM micrograph and corresponding selected area electron diffraction (SAED) of the films, respectively, which can directly obtain insight into the structural evolution caused by Ti/Al co-doping. In the film deposited at 1 A (Fig. 3a), only a typical amorphous granular structure with diffuse hallos in the diffraction pattern is observed, illustrating that the doped Ti (2.5 at.%) and Al (0.7 at.%) atoms mainly disperse in the amorphous carbon matrix. As the sputtering current is 1.5 A (Fig. 3b), the very weak crystalline diffraction rings could be distinguished from the SAED, but the lattice fringes have yet to be observed directly due to the poor crystallinity and low fraction of formed titanium carbide in the film which has been confirmed by XPS (Fig. 2b). With further increasing the sputtering current to 2.5 A (Fig. 3c), the sharp crystalline diffraction rings also indicate the existence of polycrystalline phases with diameter about 3–5 nm, which are identified to be the (111), (200), (220) and (222) reflections of cubic TiC crystallites. The case deposited at 3 A (Fig. 3d) is similar to that at 2.5 A, but noted that the obvious bright nano-strips are generated, which may be originated from pure and oxidized Al nanoclusters separated from the DLC matrix due to the excess Al concentration [18].

Fig. 4 shows the change of residual compressive stress and mechanical properties of Ti/Al-DLC films with sputtering current. As the sputtering current changes from 1 to 1.5 A, the residual compressive stress decreases significantly. During this stage, the co-doped Ti/Al atoms are uniformly dissolved in the amorphous carbon matrix and do not form the nano-crystalline carbides. Especially, previous reports [6,22–24] have proposed that the doped Ti and Al could play a pivot site to relax the structures caused by the bond angle and bond length distortions, resulting in the reduction of residual stress. Therefore, the minimal residual compressive stress of 0.41 ± 0.05 GPa is found in the film deposited at the current of 1.5 A. Beyond of the current 1.5 A, the residual stress rapidly increases and reaches to the maximal value of 1.36 ± 0.003 GPa at the current of 2.5 A. This phenomenon can be referred to the forma-



**Fig. 2.** (a) Al 2p and (b) C 1s XPS spectra, and (c) the deconvolution of the XPS C 1s peak for the film deposited at 1.5 A; (d) Raman spectra, (e) spectra fitting results for the film deposited at 1 A and (f) the corresponding  $I_D/I_G$  ratio, G peak position and  $G_{FWHM}$  of Ti/Al-DLC films deposited at different sputtering currents and using CH<sub>4</sub> as source gas.



**Fig. 3.** TEM micrograph and corresponding SAED pattern of Ti/Al-DLC films deposited at the sputtering currents of (a) 1, (b) 1.5, (c) 2.5 and (d) 3 A, respectively.

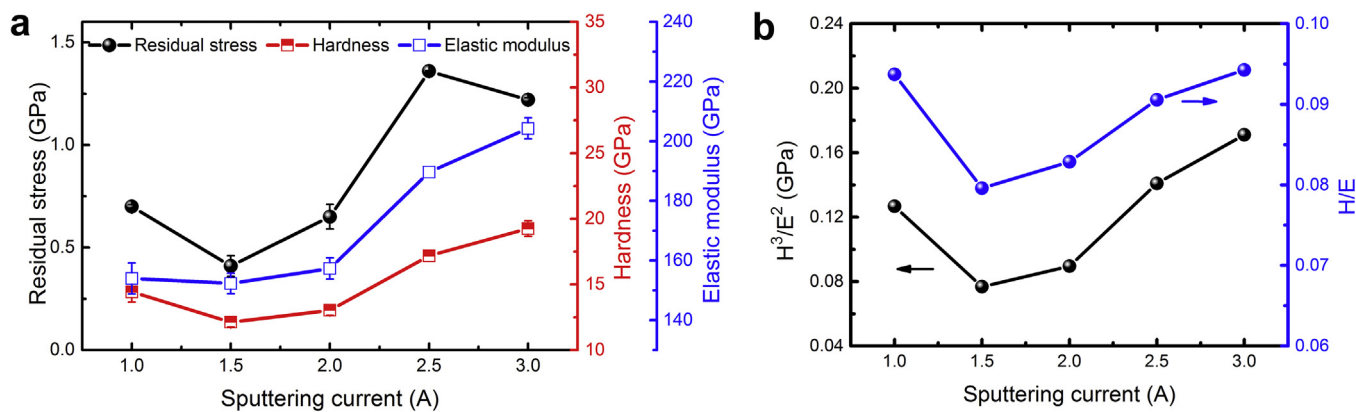


Fig. 4. (a) Residual compressive stress, hardness, elastic modulus and (b) H/E and  $H^3/E^2$  of Ti/Al-DLC films as a function of sputtering current.

tion and growth of titanium carbide nanocrystallites and aluminum oxide, which enhance the local bond distortion as proved by Li et al. [16]. However, the residual stress drops to  $1.22 \pm 0.03$  GPa again in the film deposited at the current of 3 A, which is related with the segregation of aluminum oxide nanocrystallites as confirmed by the TEM analysis (Fig. 3d).

The mechanical properties exhibit a similar dependence on sputtering current ranged from 1 to 2.5 A, as shown in Fig. 4a. When the current is lower than 1.5 A, even the doped Ti/Al atoms dissolve in the carbon matrix, they deteriorate the integrity and continuity of 3D interlink of carbon network, which results in the decrease of hardness and elastic modulus. The minimal values of  $12.1 \pm 0.4$  and  $152.3 \pm 3.4$  can be found for the hardness and elastic modulus, respectively. Compared with the film at 1 A, the hardness only decreases by 15%, but it is much smaller than the discount of 41% for residual stress reduction (Fig. 4a). Further increasing the current from 1.5 to 3 A, the fraction and size of formed titanium carbide nanocrystallites increases, which effectively compensate the deterioration of mechanical properties and thus lead to the continuous increase of hardness and elastic modulus to the maximal value of  $19.3 \pm 0.6$  and  $204.3 \pm 3.6$  GPa, respectively. In order to elucidate the effect of doped Ti and Al atoms on mechanical properties, the H/E ratio correlated to the fracture toughness and  $H^3/E^2$  related to the plastic deformation [25], are also conducted. As shown in Fig. 4b, the result shows that both the evolutions of H/E ratio and  $H^3/E^2$  with sputtering current are similar to that of hardness in Fig. 4a. In particular, when the current is higher than 1.5 A, the formation and growth of brittle titanium carbide nanocrystallites have no deterioration on the toughness, both the H/E and  $H^3/E^2$  increase monotonously. Since it is empirically known that high H/E and  $H^3/E^2$  ratios suggest the good toughness of the film, our result here implies the improved film toughness mainly attributes to the benefits from the increased ductile Al nanocrystallites and structural graphitization in the films.

### 3.2. Dependence of Ti/Al-DLC films on source gas $C_2H_2$ or $CH_4$

Because the carbonaceous gas directly affects the structure and properties of DLC matrix, we here select  $C_2H_2$  as the gas precursors for comparison with in the case using  $CH_4$ , and to study the dependence of Ti/Al-DLC films on source gas. The detailed process parameters are given as case 2 in Table 1. Fig. 5 shows that the evolutions of Ti/Al/C concentrations of the deposited films as a function of sputtering current are similar to that in  $CH_4$  case (Fig. 1). However, the differences are that the film thickness using  $C_2H_2$  (702–1313 nm) is much thicker (see Fig. 1S in Supporting information), while the concentrations of doped Ti (0–3.9 at.%) and Al (0–7.3 at.%) are much lower than that using  $CH_4$ , which are related

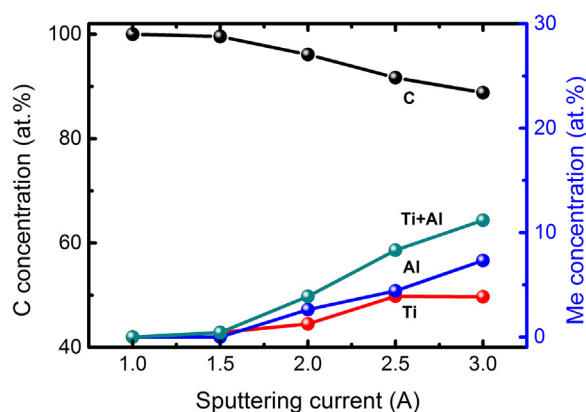
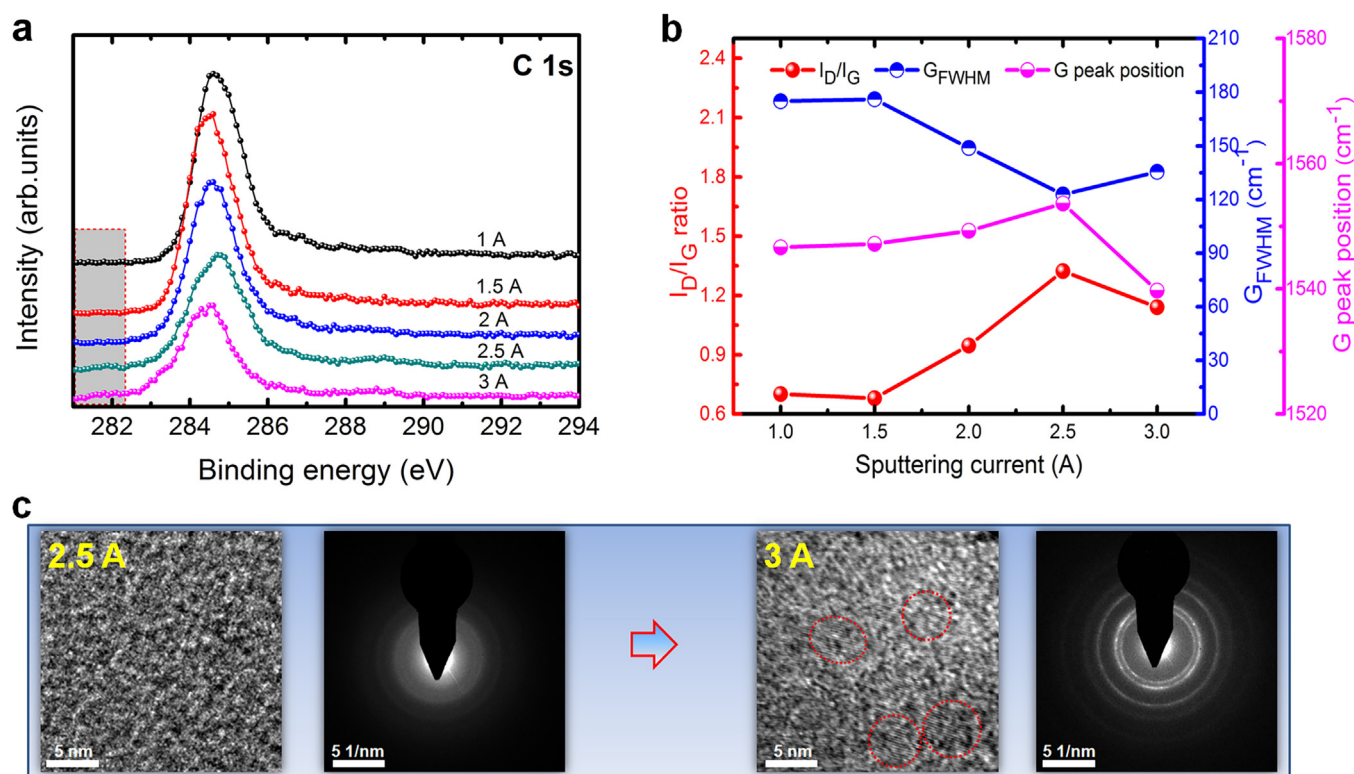


Fig. 5. Compositions of the Ti/Al-DLC films as a function of sputtering current using  $C_2H_2$  as source gas.

with higher C/H ratio of  $C_2H_2$  gas. In addition, for the film deposited at the sputtering current of 1 A, both Ti and Al atoms cannot be detected by XPS due to the existed target poisoning. Beyond of current 1 A, the target poisoning decreases due to the increased target power and more Ti/Al concentration is observed. At the current of 3 A, the doped Ti and Al concentrations are 3.9 and 7.3 at.%, respectively.

Compared to the  $CH_4$  case, XPS spectra shows that although the doped Al also exists in the form of pure Al clusters and oxidation state (see Fig. 2S in Supporting information), the small shoulder peak for C–Ti bonds starts to appear until the sputtering current is 2.5 A, as illustrated in Fig. 6a. This correlates with the Ti concentration of 3.9 at.%. With further increasing the current to 3 A, the intensity of C–Ti peak increases obviously, indicating higher fraction of formed titanium carbide phases. However, as the current is less than 2.5 A, the absence of shoulder peak for C–Ti bonds suggests that, the doped Ti atoms have no interaction with carbon atoms to form titanium carbide, which are mainly dispersed in amorphous carbon matrix.

The broad asymmetric scattering curve observed from the Raman spectra (see Fig. 3S in Supporting information), also indicates the typical characteristics of DLC film [1]. Furthermore, the fitted results in Fig. 6b show that with increasing the sputtering current, both the  $I_D/I_G$  and G peak position increase firstly and then follow by a decrease, which are contrast to the behavior of the  $G_{FWHM}$ . This results reveal that changing the sputtering current from 1 to 3 A enables the  $sp^2$  content in Ti/Al co-doped films to increase at first and then decrease; the maximal  $sp^2$  content is obtained in the case of 2.5 A. Due to the catalyst effect proposed by Dai et al. [26], the doped Ti atoms promote the graphitization of DLC



**Fig. 6.** XPS, Raman and TEM results of Ti/Al-DLC films deposited at different sputtering currents and using  $C_2H_2$  as source gas: (a) C 1s XPS spectra; (b) the fitted results of Raman spectrum including corresponding  $I_D/I_G$  ratio, G peak position and  $G_{FWHM}$  as function of sputtering current; (c) TEM micrograph and corresponding SAED pattern of the films deposited at the sputtering current of 2.5 and 3 A, respectively.

films, and also tend to bond with  $sp^2$ -C because of its lower binding energy compared with that of  $sp^3$ -C. But the doped Al as ductile element mainly contributes to the increase of  $sp^2$ -C [18]. As a result, when the sputtering current increases from 1 to 2.5 A, the doped Al and Ti with low concentrations causes the graphitization simultaneously for Ti/Al-DLC films with  $C_2H_2$  gas. However, when the current reaches to 3 A, although Al doping promotes the increase of  $sp^2$ -C content, Ti atoms with higher concentration evolve to bond with many  $sp^2$ -C and form the nanocrystalline carbides, inducing the total reduction of  $sp^2$ -C content. This is different to the  $CH_4$  case, in which the doped Al dominates the evolution of hybridized carbon structure (Fig. 2).

The representative TEM micrograph and corresponding SAED of the films deposited at the sputtering current of 2.5 and 3 A using  $C_2H_2$  as source gas are given in Fig. 6c. In case of current at 2.5 A, the weak crystalline diffraction rings with no lattice fringes are seen, which is essentially same to the film deposited at 1.5 A using  $CH_4$  (Fig. 3b). With further increasing the current to 3 A, the noticeable diffraction patterns emerge in the SAED and the nanoscaled polycrystalline TiC phases with diameter of 4–6 nm embed in the amorphous carbon matrix.

Fig. 7a gives the evolution of residual compressive stress and mechanical properties as a function of the sputtering current using  $C_2H_2$  as source gas, which have different behaviors to the films deposited using  $CH_4$ . As the current increases from 1 to 2.5 A, the compressive stress drops dramatically from  $2.39 \pm 0.2$  to  $1.28 \pm 0.1$  GPa. If one keeps in mind the minimal value of stress obtained in Fig. 4, the minimal stress of  $1.28 \pm 0.1$  GPa presently is much higher as a consequence of the higher fractions of C–C distorted structures in the film. However, further increasing the current to 3 A brings the slight increase of residual stress, because the doped Ti atoms start to bond with carbon atoms forming hard titanium carbide nanocrystallites (Fig. 6c).

The mechanical properties exhibit the similar trend to that of stress in Fig. 7a. The minimal hardness of  $13.1 \pm 0.3$  GPa and elastic modulus of  $140 \pm 1.4$  GPa are obtained, as the current is 2.5 A. According to the Raman and XPS results, the films tend to be graphitized due to the synergistic catalyst effect of doped Ti and Al atoms at current range of 1–2.5 A, resulting in the hardness reduction obviously. However, when the current is higher than 2.5 A, the hardness increases again due to the generated hard titanium carbide nanocrystallites and the decreased  $sp^2$  content in carbon matrix. Therefore, the film deposited at 3 A shows higher hardness of  $14.2 \pm 0.3$  GPa and elastic modulus of  $165 \pm 2.7$  GPa than that at 2.5 A, respectively. In addition, the  $H/E$  and  $H^3/E^2$  ratios with sputtering current decrease monotonously in Fig. 7b, indicating the damage of toughness. This behavior is related with the deterioration of integrity and continuity of carbon network and the formation of titanium carbide nanocrystallites during such small amount of Ti/Al co-doping range, while the ductile Al concentration is not high enough to retain the toughness compared with the films using  $CH_4$  (Fig. 4b).

### 3.3. Dependence of Ti/Al-DLC films on bias voltage

Ma et al. [27] and Marks [28] have indicated that the incident energies of carbon ions make important influence on structural properties of DLC films. In addition, our results of case 2 listed in Table 1 reveal the film (2.5 A,  $C_2H_2$ ) exhibiting the better combination of residual stress and mechanical properties. Therefore, based on the case 2, the incident energies of carbon ions and Ti/Al atoms are modified in this section by changing the negative pulsed bias voltage of substrate from 0 to  $-200$  V. The evolution of structure and properties of deposited Ti/Al-DLC films as a function of the bias voltage are proceeded. The detailed process parameters are seen in case 3 of Table 1.

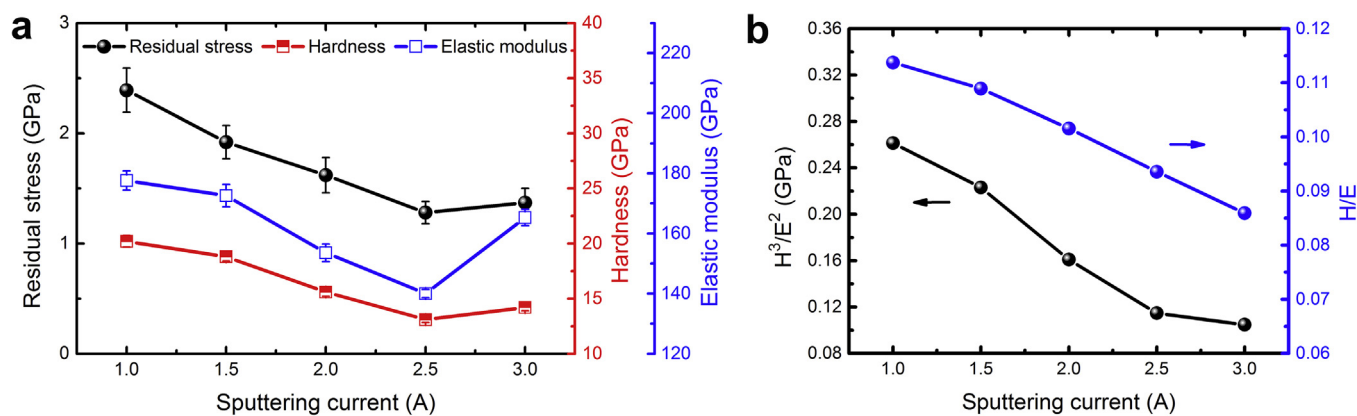


Fig. 7. (a) Residual compressive stress, hardness, elastic modulus and (b) H/E and H<sup>3</sup>/E<sup>2</sup> of Ti/Al-DLC films as a function of sputtering current using C<sub>2</sub>H<sub>2</sub> as source gas.

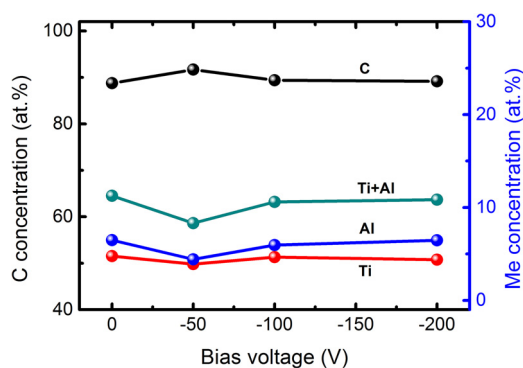


Fig. 8. Variations of Ti/Al/C concentrations in Ti/Al-DLC films deposited at different substrate bias voltages.

The film thickness is about  $1200 \pm 50$  nm regardless of the changes in bias voltage (see Fig. 4S in Supporting information). However, both the concentrations of Ti and Al decrease slightly and then increase to a stable level, which is opposite to the behavior of C concentration, as shown in Fig. 8. Namely, the obtained minimal concentration of Ti and Al is 3.9 at.% and 4.4 at.%, respectively, for the bias of -50 V. Comparing to accelerate the Ti and Al atoms, increasing the bias voltage benefits the bombardment of carbon

ions easier, causing the small decrease in Ti and Al concentrations. However, further increasing the bias promotes the re-sputtering phenomenon of deposited carbon ions from substrate [29], resulting in the slight decrease of C concentration again.

By the analysis of XPS spectra, it can be seen that for each case, the C 1s spectra can be divided into four peaks for C–C/C–H, C–O, C=O and C–Ti, respectively (see Fig. 5S in Supporting information), suggesting that the doped Ti atoms interacts with carbon atoms to form titanium carbides, while the Al atoms also exist in the form of pure and aluminum oxides states. This indicates that changing bias voltage in range of 0 to -200 V does not affect the chemical state of deposited Ti/Al co-doped DLC films to a great extent. Fig. 9 shows the TEM micrographs and corresponding SAED patterns for the Ti/Al-DLC films deposited at the bias voltage of 0, -50, -100 and -200 V. It clearly shows that the polycrystalline diffraction rings in the selected diffraction diagram exist for each case, indicating the formed TiC nanocrystallite phases, which is in agreement with the XPS results. At the bias voltage of -100 V, the magnified image also demonstrates the formed TiC nanocrystallites embedded in the amorphous carbon matrix. But in case of -50 V, the TiC lattice fringes cannot be observed due to the lower Ti concentration shown in Fig. 8.

The broad asymmetric Raman scattering curves in Fig. 6S of Supporting information also suggest the typical characteristics of amorphous carbon film. Especially, the intensity of Raman spec-

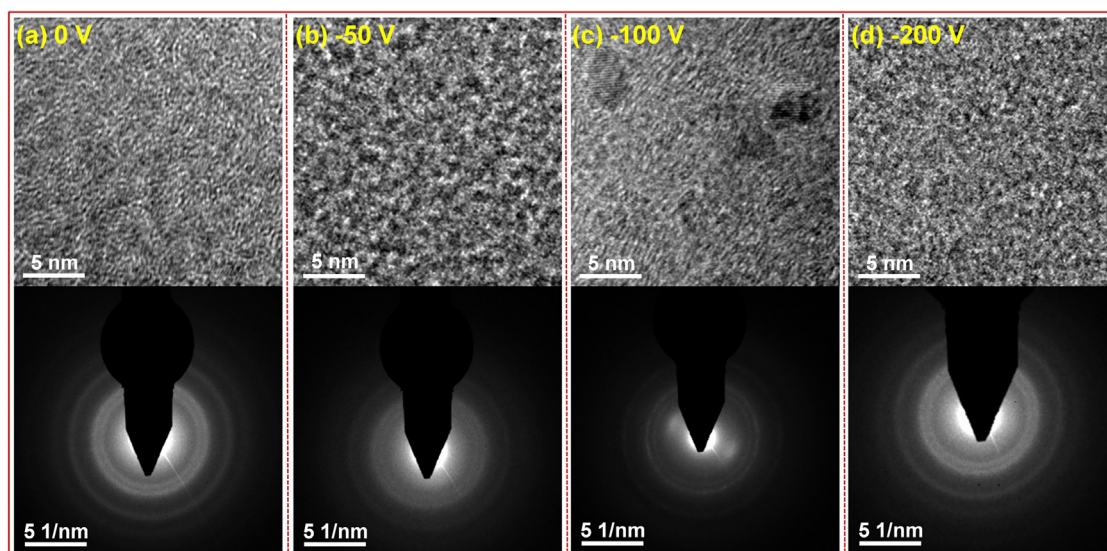


Fig. 9. TEM micrograph and corresponding SAED pattern of Ti/Al-DLC films deposited at different bias voltages of (a) 0, (b) -50, (c) -100 and (d) -200 V, respectively.

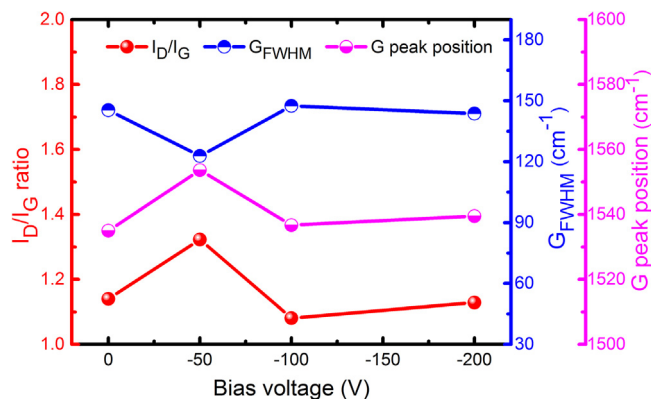


Fig. 10. Corresponding  $I_D/I_G$  ratio, G peak position and  $G_{FWHM}$  of Ti/Al-DLC films deposited at the bias voltage of 0, -50, -100 and -200 V, respectively.

tra increases slightly and follows by a small decrease due to the evolution of C concentration in films. Furthermore, the  $I_D/I_G$  and G peak position in Fig. 10 illustrate the similar trend to the peak intensity as a function of bias voltage, except the  $G_{FWHM}$  showing the contrary behavior. Specifically, at the bias of -50 V, the maximal values of  $I_D/I_G$  and G peak position are 1.32 and  $1553.6 \text{ cm}^{-1}$  respectively, while the minimal  $G_{FWHM}$  value is  $122.8 \text{ cm}^{-1}$ . Taking into account the composition and combined Raman analysis, it can be said that the  $\text{sp}^2\text{-C}$  content in the films increases firstly and then decreases as the bias voltage changes from 0 to -200 V, and the film deposited at -50 V owns the maximal  $\text{sp}^2\text{-C}$  content. Such behavior of bond structure is interpreted by the catalyst effect of Al and formation of titanium carbide phases with the co-doped Ti/Al concentrations, which acts the complicated synergistic contribution to the film structure.

The evolution of residual compressive stress and mechanical properties of Ti/Al-DLC films under different bias voltages are shown in Fig. 11. Dependent upon the changes of atomic bond structure in above Raman results, it is not surprising that the maximal stress of  $1.28 \pm 0.1 \text{ GPa}$  is found at the bias voltage of -50 V attributing to the increased incident energy of carbon ions. Further increasing the bias to -200 V, although the structure ordering decreases, the local relaxation of distortion originated from bond length and bond angles occurs due to the heating effect caused by the increased incident energy and thus leads to the reduction of residual stress, which consistent well with the molecular dynamics simulation study [27]. Different with the change of residual stress, the hardness and elastic modulus exhibit the contrast way, as shown in Fig. 11a. Comparing with this result and the structural analysis, it can be concluded that the mechanical properties

of Ti/Al-DLC film in such doping range are mainly dominated by the feature of carbide crystallites. Moreover, the evolution of  $H^3/E^2$  and  $H/E$  ratios, as shown in Fig. 11b, demonstrate the film toughness can also be understood by the synergistic effect from the carbon atomic bond and the formed small amount of titanium carbide crystallites in films. In particular, the combined superior properties for Ti/Al-DLC films including low residual stress, high hardness, as well as the good toughness, can be easily tailored by varying the sputtering current, carbonaceous precursor gas, and substrate bias voltage during the facile PVD technologies, which provide the new route to design and develop the DLC films with high performance based on the synergistic effect of co-doped metal elements for next wear resistant applications.

#### 4. Conclusions

Ti/Al co-doped DLC films were deposited by a homemade hybrid ion beam system combined with a DC magnetron sputtering source and a linear ion source. The dependence of microstructure, residual compressive stress and mechanical properties on the sputtering current, source gas and bias voltage, were investigated systematically. Results could be summarized as the following:

- (1) For case 1 using  $\text{CH}_4$  as source gas, as the sputtering current increased from 1 to 1.5 A, both the co-doped Ti and Al atoms dissolved in the amorphous carbon matrix following the structural graphitization, which decreased the residual stress, hardness and toughness. As the current was 1.5 A, the minimal residual stress and hardness were  $0.41 \pm 0.05 \text{ GPa}$  and  $12.1 \pm 0.4 \text{ GPa}$ , respectively. With further increasing the current to 2.5 A, the doped Al atoms existed in form of pure and oxidized Al clusters, while the Ti atoms formed the hard titanium carbide nanocrystallites and embedded in the amorphous carbon interlinkages, resulting in higher residual stress and hardness without the deterioration of toughness due to synergistic effect from high ductile Al concentration. However, when the current further reached to 3 A, the separation of aluminum oxide nanocrystallites from DLC matrix led to the reduction of residual stress.
- (2) For case 2 using  $\text{C}_2\text{H}_2$  as source gas, when the precursor gas  $\text{CH}_4$  was replaced by  $\text{C}_2\text{H}_2$  for DLC deposition, the relative concentrations of co-doped Ti and Al were decreased to a great extent, suppressing the emerge of formed titanium carbide phase in films. The mechanical properties showed similar dependence upon the sputtering current as case 1. However, different with the cause for stress evolution in case 1, the residual stress in case 2 was closely related with the synergistic graphitization effect originated from small amount of concentration for doped Ti and Al atoms in film. Specifically, the minimal residual stress

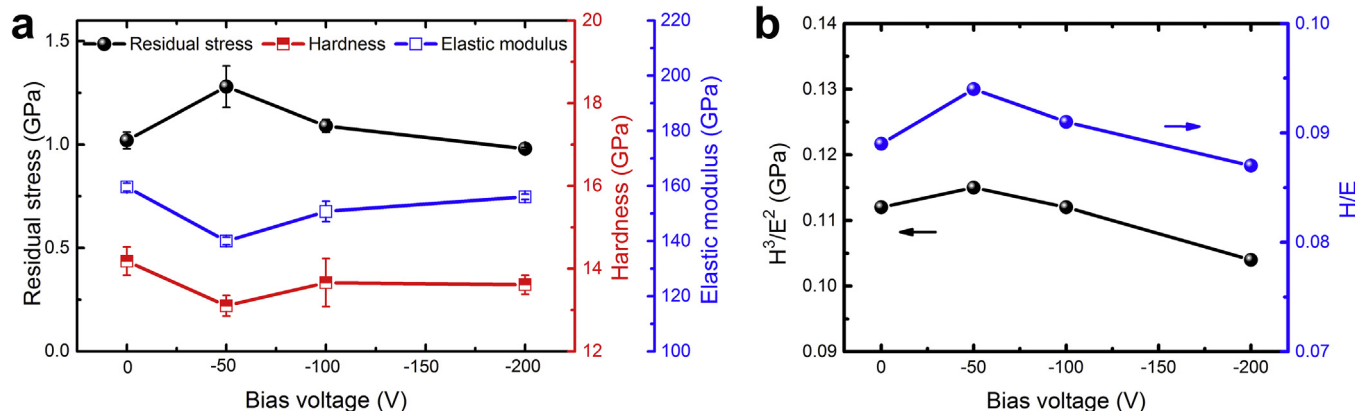


Fig. 11. (a) Residual compressive stress, hardness and elastic modulus, (b)  $H^3/E^2$  and  $H/E$  of Ti/Al-DLC films deposited at different bias voltages.

of  $1.28 \pm 0.1$  GPa was achieved as the current was 2.5A, which was much higher than that in same current of  $\text{CH}_4$  case, because of higher fractions of C–C distorted structures in this case 2.

- (3) For case 3, when the sputtering current was optimized at 2.5 A, all the films deposited at the bias voltage in range of 0 to  $-200$  V showed the formation of hard titanium carbide phase. However, because increasing bias voltage made more contribution to the enhancement of incident energy for carbon ions comparing to that of Ti and Al atoms, the concentration of doped Ti and Al in films decreased slightly and then increased. The combined structural and atomic bond analysis revealed that the residual stress was the main consequence of the structural relaxation originated by the carbon ions, while the mechanical properties were mainly dominated by the feature of the titanium carbide.

## Acknowledgments

This research was supported by the National Natural Science Foundation of China (51402319, 51522106), State Key Project of Fundamental Research of China (2013CB632302), 2016 Korea–China Young Scientist Exchange Program and Public Project of Zhejiang Province (2016C31121).

## Appendix A. Supplementary data

Supplementary data associated with this article can be found, in the online version, at <http://dx.doi.org/10.1016/j.apsusc.2017.02.254>.

Thickness of the Ti/Al-DLC films as a function of sputtering current using  $\text{C}_2\text{H}_2$  as source gas (Fig. 1S); Al 2p XPS spectra of the Ti/Al-DLC films deposited at different sputtering currents using  $\text{C}_2\text{H}_2$  as source gas (Fig. 2S); Raman spectra of Ti/Al-DLC films deposited at different sputtering currents using  $\text{C}_2\text{H}_2$  as source gas (Fig. 3S); Variations of thickness in Ti/Al-DLC films under different substrate bias voltages (Fig. 4S); Typical C 1s XPS spectra of Ti/Al-DLC films deposited at different bias voltages (Fig. 5S); Raman spectra of Ti/Al-DLC films deposited at the bias voltage of 0,  $-50$ ,  $-100$  and  $-200$  V, respectively (Fig. 6S).

## References

- [1] J. Robertson, Diamond-like amorphous carbon, *Mater. Sci. Eng.* 37 (2002) 129–281.
- [2] K. Bewilogua, D. Hofmann, History of diamond-like carbon films—from first experiments to worldwide applications, *Surf. Coat. Technol.* 242 (2014) 214–225.
- [3] W. Dai, A.Y. Wang, Deposition and properties of Al-containing diamond-like carbon films by a hybrid ion beam sources, *J. Alloys Compd.* 509 (2011) 4626–4631.
- [4] C.S. Lee, K.R. Lee, K.Y. Eun, K.H. Yoon, J.H. Han, Structure and properties of Si incorporated tetrahedral amorphous carbon films prepared by hybrid filtered vacuum arc process, *Diamond Relat. Mater.* 11 (2002) 198–203.
- [5] A.Y. Wang, H.S. Ahn, K.R. Lee, J.P. Ahn, Unusual stress behavior in W-incorporated hydrogenated amorphous carbon films, *Appl. Phys. Lett.* 86 (2005), 111902-1–3.
- [6] X. Li, L. Sun, P. Guo, P. Ke, A. Wang, Structure and residual stress evolution of Ti/Al, Cr/Al or W/Al co-doped amorphous carbon nanocomposite films: insights from ab initio calculations, *Mater. Des.* 89 (2016) 1123–1129.
- [7] X. Li, P. Guo, L. Sun, A. Wang, P. Ke, Ab initio investigation on Cu/Cr codoped amorphous carbon nanocomposite films with giant residual stress reduction, *ACS Appl. Mater. Interfaces* 7 (2015) 27878–27884.
- [8] X. Pang, J. Hao, P. Wang, Y. Xia, W. Liu, Effects of bias voltage on structure and properties of TiAl-doped a-C:H films prepared by magnetron sputtering, *Surf. Interface Anal.* 43 (2011) 677–682.
- [9] X.Q. Liu, J. Yang, J.Y. Hao, J.Y. Zheng, Q.Y. Gong, W.M. Liu, A nearly frictionless and extremely elastic hydrogenated amorphous carbon film with self-assembled dual nanostructure, *Adv. Mater.* 24 (2012) 4614–4617.
- [10] A.Y. Wang, K.R. Lee, J.P. Ahn, J.H. Han, Structure and mechanical properties of W incorporated diamond-like carbon films prepared by a hybrid ion beam deposition technique, *Carbon* 44 (2006) 1826–1832.
- [11] W. Yang, Y. Guo, D. Xu, J. Li, P. Wang, P. Ke, A. Wang, Microstructure and properties of (Cr:N)-DLC films deposited by a hybrid beam technique, *Surf. Coat. Technol.* 261 (2015) 398–403.
- [12] Š. Meškinis, R. Gudaitis, V. Kopustinskas, S. Tamulevičius, Electrical and piezoresistive properties of ion beam deposited DLC films, *Appl. Surf. Sci.* 254 (2008) 5252–5256.
- [13] A. Anders, Plasma and ion sources in large area coating: a review, *Surf. Coat. Technol.* 200 (2005) 1893–1906.
- [14] I.V. Bordenjuk, O.A. Panchenko, S.V. Sologub, I.G. Brown, Development of additional magnetron discharge in the drift region of an ion source with closed electron drift, *Probl. Atom. Sci. Technol.* 6 (2008) 168–170.
- [15] W. Yang, P. Ke, Y. Fang, H. Zheng, A. Wang, Microstructure and properties of duplex (Ti:N)-DLC/MAO coating on magnesium alloy, *Appl. Surf. Sci.* 270 (2013) 519–525.
- [16] X. Li, P. Guo, L. Sun, X. Zuo, D. Zhang, P. Ke, A. Wang, Ti/Al co-doping induced residual stress reduction and bond structure evolution of amorphous carbon films: an experimental and ab initio study, *Carbon* 111 (2017) 467–475.
- [17] S. Zhou, L. Wang, Z. Lu, Q. Ding, S.C. Wang, R.J.K. Wood, Q. Xue, Tailoring microstructure and phase segregation for low friction carbon-based nanocomposite coatings, *J. Mater. Chem.* 22 (2012) 15782–15792.
- [18] W. Dai, P. Ke, A. Wang, Influence of bias voltage on microstructure and properties of Al-containing diamond-like carbon films deposited by a hybrid ion beam system, *Surf. Coat. Technol.* 229 (2013) 217–221.
- [19] H.M. Liao, R.N.S. Sodhi, T.W. Coyle, Surface composition of AlN powders studied by xray photoelectron spectroscopy and bremsstrahlungexcited Auger electron spectroscopy, *J. Vac. Sci. Technol.* 11 (1993) 2681–2686.
- [20] G. Zhang, P. Yan, P. Wang, Y. Chen, J. Zhang, The preparation and mechanical properties of Al-containing a-C: H thin films, *J. Phys. D Appl. Phys.* 40 (2007) 6748–6752.
- [21] K. Baba, R. Hatada, Deposition and characterization of Ti- and W-containing diamond-like carbon films by plasma source ion implantation, *Surf. Coat. Technol.* 169–170 (2003) 287–290.
- [22] J.H. Choi, S.C. Lee, K.R. Lee, A first-Principles study on the bond characteristics in carbon containing Mo Ag, or Al impurity atoms, *Carbon* 46 (2008) 185–188.
- [23] X. Li, D. Zhang, K.R. Lee, A. Wang, Effect of metal doping on structural characteristics of amorphous carbon system: a first-principles study, *Thin Solid Films* 607 (2016) 67–72.
- [24] X. Li, P. Ke, A. Wang, Probing the stress reduction mechanism of diamond-like carbon films by incorporating Ti, Cr, or W carbide-forming metals: ab initio molecular dynamics simulation, *J. Phys. Chem. C* 119 (2015) 6086–6093.
- [25] C.A. Charitidis, Nanomechanical and nanotribological properties of carbon-based thin films: a review, *Int. J. Refract. Met. Hard Mater.* 28 (2010) 51–70.
- [26] W. Dai, P. Ke, M. Moon, K.R. Lee, A. Wang, Investigation of the microstructure, mechanical properties and tribological behaviors of Ti-containing diamond-like carbon films fabricated by a hybrid ion beam method, *Thin Solid Films* 520 (2012) 6057–6063.
- [27] T. Ma, Y. Hu, H. Wang, X. Li, Microstructural and stress properties of ultrathin diamondlike carbon films during growth: molecular dynamics simulation, *Phys. Rev. B* 75 (2007) 035425-1-8.
- [28] N.A. Marks, Thin film deposition of tetrahedral amorphous carbon: a molecular dynamics study, *Diamond Relat. Mater.* 14 (2005) 1223–1231.
- [29] X. Li, P. Ke, H. Zheng, A. Wang, Structural properties and growth evolution of diamond-like carbon films with different incident energies: a molecular dynamics study, *Appl. Surf. Sci.* 273 (2013) 670–675.